

UNCLASSIFIED

AD NUMBER
AD801622
NEW LIMITATION CHANGE
TO Approved for public release, distribution unlimited
FROM Distribution authorized to U.S. Gov't. agencies and their contractors; Critical Technology; AUG 1966. Other requests shall be referred to Space Systems Division, ATTN: SSTRT, Los Angeles, CA.
AUTHORITY
SAMSO ltr dtd 24 Jan 1972

THIS PAGE IS UNCLASSIFIED

80162

Compressible Flow through a Porous Plate

AUGUST 1966

~~by~~ **A. EMANUEL and J. F. JONES**
~~of the~~ **Aerodynamics and Propulsion Research Laboratory**
Laboratory Division
Laboratory Operations
AIR FORCE CORPORATION

Prepared for **BALLISTIC SYSTEMS AND SPACE SYSTEMS DIVISIONS**
AIR FORCE SYSTEMS COMMAND
LOS ANGELES AIR FORCE STATION
Los Angeles, California

Air Force Report No.
SSD-TR-66-165

Aerospace Report No.
TR-669(6240-20)-15

COMPRESSIBLE FLOW THROUGH A POROUS PLATE

Prepared by

G. Emanuel and J. P. Jones
Aerodynamics and Propulsion Research Laboratory

Laboratories Division
Laboratory Operations
AEROSPACE CORPORATION

August 1966

Prepared for

BALLISTIC SYSTEMS AND SPACE SYSTEMS DIVISIONS
AIR FORCE SYSTEMS COMMAND
LOS ANGELES AIR FORCE STATION
Los Angeles, California

FOREWORD

This report is published by the Aerospace Corporation, El Segundo, California, under Air Force Contract No. AF 04(695)-669.

This report, which documents research carried out from January 1966 to July 1966, was submitted on 9 September 1966 to Captain Robert F. Jones, SSTRT, for review and approval.

The authors acknowledge the helpful discussions with T. A. Jacobs and W. S. Lewellen of Aerospace Corporation. They also wish to acknowledge the assistance of L. Plansky in the preparation of some of the figures.

Information in this report is embargoed under the U. S. Export Control Act of 1949, administered by the Department of Commerce. This report may be released by departments or agencies of foreign governments with which the United States has defense treaty commitments. Private individuals or firms must comply with Department of Commerce export control regulations.

Approved

M. T. Weiss
for J. G. Logan, Director
Aerodynamics and Propulsion
Research Laboratory

Publication of this report does not constitute Air Force approval of the report's findings or conclusions. It is published only for the exchange and stimulation of ideas.

Robert F. Jones
Robert F. Jones, Capt., USAF
Space Systems Division
Air Force Systems Command

ABSTRACT

A simple one-dimensional theory is given for the steady, compressible, adiabatic flow of a perfect gas through a porous plate. The Dupuit-Forchheimer relation, valid for incompressible flow, is replaced by an isentropic compression when the gas enters the plate and a non-isentropic sudden enlargement process when it exits. A generalized form of Darcy's equation is used that is applicable to adiabatic flow. It retains the convective term, which is necessary if the flow is compressible. An important consequence of this study is that the Mach number at the downstream surface may be much smaller than unity, even when the flow through the plate is choked. As the pressure ratio across the plate decreases, the flow remains choked, but the downstream Mach number increases. In fact, this Mach number will be greater than unity for a sufficiently small pressure ratio, in which case the downstream flow is supersonic. Thus, a wide range of downstream Mach numbers from subsonic to supersonic is possible, even though the flow is choked. For incompressible flow, the volumetric flow rate varies linearly with the pressure differential across the plate. The equivalent compressible relation is shown to consist of a plot of upstream Mach number versus the pressure ratio across the plate. The incompressible result can also be shown on this plot; it differs from the compressible one, except when the plate is thick.

CONTENTS

FOREWORD	ii
ABSTRACT	iii
NOMENCLATURE	vii
INTRODUCTION	1
FORMULATION	5
$M_3 < 1$ AND $M_3 \rightarrow 1$ ANALYSIS	8
MOMENTUM	12
The Isothermal Case	12
The Adiabatic Case	14
The Compressible Momentum Equation	17
CHOKED FLOW: $M_3 = 1$	21
DISCUSSION	24
REFERENCES	29
APPENDIX	31

FIGURES

1.	Flow Schematic for a Porous Plate inside a Duct	33
2.	Mollier Diagram for Subsonic Flow through a Porous Plate	33
3.	$G_1(M^2)$ vs M^2 ; $\gamma = 7/5$	34
4.	\bar{M}_4^2 vs β ; $\gamma = 7/5$	35
5.	$(\overline{p_1 M_1 / p_4})^2$ vs \bar{M}_4^2 ; $\gamma = 7/5$	36
6.	Comparison of the Terms in Equation (10b); $\gamma = 7/5$, $M_1^2 = 0.01$.	37
7.	$F(M^2)$ vs M^2 ; $\gamma = 7/5$	38
8.	bL vs M_1^2 / β^2 when $M_3 = 1$; $\gamma = 7/5$	39
9.	$(\overline{p_4 / p_1})^2$, $[(p_4 / p_1)^*]^2$, and $(\underline{p_4 / p_1})^2$ vs bL ; $\gamma = 7/5$	40
10.	Mollier Diagram for Choked Flow Through a Porous Plate.	41
11.	M_1^2 vs $(p_4 / p_1)^2$ for $bL = 1, 10, 10^2$; $\beta^2 = 0.2$, $\gamma = 7/5$	42

NOMENCLATURE

$b,$	drag coefficient;
$B_0,$	Darcy's constant;
$d,$	average pore diameter;
$f_i,$	functions defined by Eqs. (18) and (20);
$F(M^2)$	function defined by Eq. (14);
$G_i(M^2),$	Mach number functions;
$h,$	enthalpy;
$L,$	porous plate thickness;
$M,$	Mach number;
$p,$	pressure;
$R,$	gas constant;
$R_d,$	Reynolds number;
$s,$	entropy;
$T,$	temperature;
$u,$	velocity;
$x,$	distance in the direction of flow;
$X,$	drag;
$\beta,$	porosity;
$\gamma,$	ratio of specific heats;
$\eta,$	viscosity;
$\rho,$	density.

INTRODUCTION

For the vast majority of problems concerning flow of a liquid in a porous medium, the fluid is considered incompressible (or slightly compressible) and the convective terms are neglected. For most classes of problems, such as ground water and seepage flow, these assumptions are not unreasonable, and have been used in investigations of this type [1, 2]. When the fluid is a compressible gas subject to large pressure gradients, such assumptions are no longer valid, and a different methodology must be applied. The purpose of this paper is to develop a simple theory for one-dimensional, compressible flow of a gas through a porous plate.

This work was initially motivated by recent developments in high speed reentry technology. In an attempt to simulate ablation off the surface of a reentry vehicle, Hartunian and Spencer [3] introduced the concept of massive blowing in wind tunnel experiments using models of a porous material such as sintered stainless steel. A substantial pressure difference, usually greater than 100 to 1, is established across the wall of the model. A large mass flow rate through the wall ensues and appreciable density gradients occur.

Our interest here is the interaction of the injected gas with the porous material, not the external flow field of the injected and free-stream gases. In order to concentrate more fully on the physics of this interaction, the following simplifying assumptions are introduced:

1. Steady, one-dimensional flow is assumed.
2. The physical model of a gas flowing in a straight, frictionless duct of constant cross section is adopted. Situated in the duct is a porous plate of uniform thickness (see Fig. 1).

3. A perfect gas is assumed with a constant value for the ratio of specific heats.
4. Continuum mechanics govern the flow.

We take as a mathematical model for the viscous flow inside the plate the formulation applicable to flow in a straight duct with friction. This description is intended to represent average flow conditions at any cross section of the plate and does not imply the assumption of a capillary model in which the pores are straight ducts transverse to the plate. The theory associated with this approach is well established and widely known. (See, for example, Shapiro [4], whose work is heavily relied upon here.) We follow [4] and use the Mach number as the independent variable, which yields a formulation that is physically elegant and mathematically simple. An important result of this approach is that momentum considerations can be dealt with separately, as has been done in the subsequent analysis.

The distinguishing feature of this analysis is the generalization of the Dupuit-Forchheimer relation [1, 2], which says that the volumetric flow rate is constant across the surface of a porous medium. The fluid thus adjusts to the smaller flow area available to it in the medium. In incompressible flow theory, this relation is used regardless of whether the fluid is entering or leaving the medium. By contrast, instead of the Dupuit-Forchheimer relation, we use the isentropic assumption when the fluid is entering the plate. On exiting, the flow is assumed to adjust to the larger available area by means of an irreversible process.

The most important consequence of this analysis is that although the flow may be choked, the Mach number at the downstream surface is generally not unity. (By choking we mean that the mass flow rate through the porous plate is a maximum.) Specifically, as the pressure ratio across the plate decreases, the flow becomes choked, but the downstream Mach number may still be much smaller than unity. As the pressure ratio further decreases, the flow remains choked, while the downstream Mach number increases. In fact, this Mach number will become greater than unity for sufficiently small pressure ratios. In other words, although the flow through the plate is choked, a wide range of downstream Mach numbers ranging from subsonic to supersonic is nevertheless possible. In addition, a limiting pressure ratio and Mach number exist beyond which solutions are no longer possible according to this theory.

Results of this work can be given as a plot of upstream Mach number versus the pressure ratio across the plate. This is equivalent, for the compressible case, to the normal incompressible relation of the volumetric flow rate versus the pressure differential across the plate. The incompressible result can also be shown on our plot; it differs from the compressible one, except when all Mach numbers are small or when the plate is thick (see below).

We formulate the problem in the following section. The case when choking does not occur is analyzed first. Momentum considerations are dealt with in a separate section and the validity of Darcy's equation for

both isothermal and adiabatic flow through the plate is discussed. The subsequent section treats the choked-flow case, while the final section discusses a number of important aspects of the theory, including the generalization of the plot of flow rate versus pressure differential.

FORMULATION

Consider one-dimensional flow of a perfect gas through a plate of uniform porosity β (see Fig. 1). The cross-sectional area of the plate is taken to be unity, consequently, the area available to the flow within the plate is β , which must be less than unity. A streamtube of fluid thus contracts in area as it enters the plate and expands in area as it leaves. These changes are assumed to occur between locations 1 and 2, and 3 and 4, respectively. Both area changes are assumed to occur in a short distance in comparison to the plate's thickness.

Upstream of the plate, the flow is at a low subsonic Mach number, i. e. , $M_1 \ll 1$, given by

$$M_1^2 = \frac{u_1^2}{\gamma(p_1/\rho_1)} = \frac{RT_1(\rho_1 u_1)^2}{\gamma P_1^2} \quad , \quad (1)$$

where u is velocity, γ is the (constant) ratio of specific heats, p is pressure, ρ is density, P is the gas constant, and T is temperature. Because $M_1 \ll 1$, the thermodynamic quantities in equation (1) differ negligibly from their stagnation values. Similarly, in all ensuing formulas we use without further statement or justification the approximation

$$1 + (\gamma - 1)M_1^2/2 \cong 1 \quad .$$

Between locations 1 and 2 we assume the area change is accomplished by means of an isentropic process; the flow is thus analogous to that in the convergent part of a nozzle. Associated with the flow is a small loss of

stagnation pressure, but this loss is minute compared with that between locations 2 and 3 and therefore is neglected.

Between locations 2 and 3 we assume the flow is adiabatic but non-isentropic due to viscous-energy dissipation.¹ Flow conditions are described by a Fanno curve, which combines the adiabatic assumption with continuity. Such a curve [4] is independent not only of the form of the drag term in the momentum equation, but of the momentum equation itself. This is an important point to bear in mind, since much of the analysis deals with properties of the Fanno curve, and is thus valid for any momentum equation.

One of the fundamental properties of a Fanno curve is that at the "nose" (see Fig. 2) the entropy is a maximum and the Mach number is unity. Associated with this is the phenomenon of choking. Specifically, when $M_2 < 1$, as is the case here, we have the condition $M_3 \leq 1$, which plays an important role in the subsequent analysis.

Between 3 and 4 we assume the area change is accomplished by a sudden enlargement, which is a non-isentropic process. When $M_3 < 1$, this is a compression, i. e. , an increasing pressure, which results in a lower Mach number at 4 than at 3. When M_3 is near unity and β is small, an entropy

¹We could also assume the flow between 2 and 3 to be isothermal. However, [4] (Chapter 6) shows that both assumptions yield similar results qualitatively and quantitatively. For experiments of long duration involving flow through a thin plate, we adopt the adiabatic assumption as the more realistic one.

increase occurs which cannot be neglected. Since this case is important, we use the more exact irreversible process throughout the analysis, even though an isentropic process would otherwise be feasible when $M_3 < 1$.

These considerations are conveniently illustrated by a Mollier diagram (Fig. 2). The ordinate is the enthalpy h , where h_0 , the stagnation enthalpy, is constant from 1 to 4, since the entire process is adiabatic. Locations 1, 2, 3, and 4 are state points on the diagram and hereafter are so designated. States 1 and 4 are connected by a Fanno curve, since these states have the same mass flux rate and h_0 . This curve is to the right of the curve passing through 2 and 3 because of the smaller mass flux per unit area. In the $\beta = 1$ limit, both curves coincide; as β decreases from unity they diverge. In Fig. 2, flow conditions between 1 and 2 are given by an isentropic subsonic expansion, flow conditions between 2 and 3 are given by the Fanno curve, while the irreversible subsonic compression occurs between 3 and 4.

Figure 2 and the process between states 3 and 4 are valid when $M_3 < 1$ and in the limit $M_3 \rightarrow 1$. When $M_3 = 1$, the flow chokes and the analysis must be altered to allow for other solutions in addition to the $M_3 \rightarrow 1$ limit. We shall first consider the $M_3 < 1$ case, along with the limit $M_3 \rightarrow 1$.

$M_3 < 1$ AND $M_3 \rightarrow 1$ ANALYSIS

States 1 and 4 are related by the Fanno curve [4]

$$M_1^2 = \left(\frac{p_4}{p_1}\right)^2 G_0(M_4^2), \quad (2a)$$

where

$$G_0(M^2) \equiv M^2 \left[1 + (\gamma - 1) M^2/2 \right].$$

States 1 and 2 are isentropically related by [4]

$$M_1^2 = \beta^2 G_1(M_2^2), \quad (2b)$$

where

$$G_1(M^2) \equiv \frac{M^2}{\left[1 + (\gamma - 1) M^2/2 \right]^{(\gamma+1)/(\gamma-1)}}.$$

States 3 and 4 are related by the momentum equation for a sudden enlargement from an area β to unit area. This equation is (see [4], problem 5.23)

$$(1 - \beta) p_3 + (\beta)(p_3 + \rho_3 u_3^2) = (1)(p_4 + \rho_4 u_4^2), \quad (3)$$

which is valid only when $M_3 < 1$, or in the limit $M_3 \rightarrow 1$. By means of the isentropic relation for p_2/p_1 and the Fanno curve relation for p_2/p_3 , equation (3) can be written as

$$\frac{(1 + \gamma \beta M_3^2)^2}{G_0 (M_3^2)} = \left(\frac{P_4}{P_1}\right)^2 \frac{(1 + \gamma M_4^2)^2}{G_1 (M_4^2)} \quad (2c)$$

The three equations (2) relate four Mach numbers, and consequently an additional relation is necessary. This is provided by conservation of momentum between states 2 and 3, which is given later.

A more convenient form for equation (2c), obtained with the aid of (2a) and (2b), is

$$\frac{M_4^2 + (\gamma - 1)M_4^4/2}{(1 + \gamma M_4^2)^2} = \frac{\beta(\beta M_3^2) + (\gamma - 1)(\beta M_3^2)^2/2}{[1 + \gamma(\beta M_3^2)]^2} \quad (4)$$

We deduce from this that $M_4^2 \leq \beta M_3^2$. From equation (3) we have

$$\frac{P_4}{P_3} = \frac{1 + \gamma(\beta M_3^2)}{1 + \gamma M_4^2} \quad (5)$$

and consequently $p_3 \leq p_4$.

A second bound on M_4 , more useful than the one above, is obtained from equation (4) and the condition $M_3 < 1$, and is

$$G_2(M_4^2) < \frac{\gamma + 1}{2} \left(\frac{\beta}{1 + \gamma\beta} \right)^2, \quad (6)$$

where

$$G_2(M^2) \equiv \frac{G_0(M^2)}{(1 + \gamma M^2)^2}.$$

Figure 3 is a plot of the $G_1(M^2)$ versus M^2 for $\gamma = (7/5)$. Thus, M_4 is bounded, where this bound, \bar{M}_4 , is obtained from (6) by replacing the inequality by an equality sign. Figure 4 shows \bar{M}_4^2 versus β for $\gamma = (7/5)$.

From equation (2a) and inequality (6), we see that $(p_1 M_1 / p_4)^2$ also has an upper bound, $(\bar{p}_1 M_1 / \bar{p}_4)^2$, which is shown as a function of \bar{M}_4^2 in Fig. 5 for $\gamma = (7/5)$. For a given value of β there is a maximum value \bar{M}_4^2 (Fig. 4), which in turn leads to a maximum value $(\bar{p}_1 M_1 / \bar{p}_4)^2$ (Fig. 5). In the limit $M_3 \rightarrow 1$, we have $M_4 = \bar{M}_4$ and $(p_1 M_1 / p_4) = (\bar{p}_1 M_1 / \bar{p}_4)$. When $M_3 = 1$, however, other solutions, which are discussed later, are also possible.

It is clear from Fig. 4 that M_4 will be small when β is small. Suppose both M_1 and M_4 are small. This does not imply that the flow is incompressible, since M_3 may still be near unity. Figure 4 further shows (when $M_3 < 1$) that large values of M_4 cannot be attained for many porous media, since β is usually usually less than 0.6.

In the limit when all Mach numbers are small, we obtain from equations (2) the simple result

$$M_1 = \beta M_2 = \beta \left(\frac{P_4}{P_1} \right) M_3 = \left(\frac{P_4}{P_1} \right) M_4, \quad (7)$$

which is used later.

MOMENTUM

The foregoing analysis is completely independent of the momentum equation applicable between states 2 and 3. For compressible flow, this equation can be written as (see [4], Chapter 8)

$$dp + dX = -\rho u \, du \quad . \quad (8)$$

The drag term is

$$dX = \frac{1}{2} b \rho u^2 \, dx \quad , \quad (9)$$

where x is distance in the direction of flow, and b is a drag coefficient with dimensions $(\text{length})^{-1}$, considered constant when any integration with respect to x is performed. Equation (9) is identical to that used in [4] (Chapter 6), with $b \equiv (4f/D)$, and was chosen, in part, for this reason. A comparison with Darcy's law (as given, for instance, in [2], p. 2) shows that $b = (2\eta/\rho u B_0)$, where B_0 is Darcy's constant and η is the viscosity of the gas. A more detailed discussion of the physical implications of the drag coefficient is given in the last section.

The Isothermal Case

Darcy's equation is universally used as the momentum equation for incompressible flow in a porous medium. Although we are primarily interested in adiabatic flow, it is useful to consider the isothermal case in order to show the relationship of Darcy's equation to the present work. We begin by presenting the usual derivation of Darcy's equation for isothermal flow, neglecting

the convective term $\rho u du$. We then present a more precise derivation, which retains the convective term and shows that Darcy's equation is not uniformly valid in the incompressible limit. Nevertheless, it is also shown that Darcy's equation usually differs negligibly from the correct momentum equation. As we shall see later, the same type of nonuniformity appears in the adiabatic case.

Consider the isothermal case neglecting $\rho u du$ and the area changes at the plate's surfaces. The area changes are included when the adiabatic case is analyzed. We therefore obtain

$$p dp = -\frac{1}{2} b p \rho u^2 dx = -\frac{1}{2} b R T_1 (\rho_1 u_1)^2 dx$$

and by integrating between 1 and 4, we obtain Darcy's equation

$$bL = \frac{p_1^2 - p_4^2}{R T_1 (\rho_1 u_1)^2} = \frac{1 - (p_4/p_1)^2}{\gamma M_1^2} \quad , \quad (10a)$$

where L is the thickness of the plate, and where equation (1) is used to obtain the second equality. The only alteration that the neglected area changes make is to introduce a β^2 factor on the right side of equation (10a)

If we now retain the $\rho u du$ term, and still assume isothermal flow, we obtain (see [4], Chapter 6)

$$bL = \frac{1}{\gamma M_1^2} - \frac{1}{\gamma M_4^2} + 2 \ln \left(\frac{M_1}{M_4} \right) \quad .$$

By means of an equation for M_4 similar to (1), this becomes

$$bL = \frac{1 - (p_4/p_1)^2}{\gamma M_1^2} + \ln (p_4/p_1)^2, \quad (10b)$$

which differs from (10a) by the logarithm term. Because of this term, Darcy's equation is not a uniformly valid approximation in the incompressible limit. (In this limit, we replace M_1^2 by equation (1).) Figure 6 shows, however, that the absolute value of the logarithm term is small compared to the value of the right side of (10a), except for exceedingly small values of $(p_4/p_1)^2$, when compressibility should not be neglected in any case.

The Adiabatic Case

Next, consider adiabatic flow from states 2 to 3, and in parallel to the preceding case, examine first equation (8) without the ρu du term. This equation can be written as

$$b \, dx = \frac{1}{\gamma} \left[\frac{1 + (\gamma - 1)M^2}{1 + (\gamma - 1)M^2/2} \right] \frac{dM^2}{M^4},$$

which becomes on integration

$$bL = \frac{1}{\gamma M_2^2} - \frac{1}{\gamma M_3^2} + \left(\frac{\gamma - 1}{2\gamma} \right) \ln \left[\frac{M_3^2 \left[1 + (\gamma - 1)M_2^2/2 \right]}{M_2^2 \left[1 + (\gamma - 1)M_3^2/2 \right]} \right] \quad (11)$$

For small Mach numbers, this can be written as (see equations (7))

$$bL = \beta^2 \frac{1 - (p_4/p_1)^2}{M_1^2} - \left(\frac{\gamma - 1}{2\gamma} \right) \ln (p_4/p_1)^2 \quad (12)$$

This equation differs from (10a) by the β^2 coefficient, which is due to the area changes, and by the logarithm term. Again, this term is small compared to the β^2 term, except at small pressure ratios. Henceforth, we refer to equation (12), without the logarithm term, as Darcy's equation.

When the $pu \, du$ term is retained, we obtain in place of equation (11) (see [4], Chapter 6)

$$bL = F(M_2^2) - F(M_3^2) \quad , \quad (13)$$

where

$$F(M^2) \equiv \frac{1}{\gamma M^2} + \left(\frac{\gamma + 1}{2\gamma} \right) \ln \left[\frac{M^2}{1 + (\gamma - 1)M^2/2} \right] \quad , \quad (14)$$

which is shown in Fig. 7 for $\gamma = (7/5)$. For comparative purposes, this figure also shows $1/\gamma M^2$, which closely approximates F for small M^2 . For small Mach numbers, equation (13) becomes

$$bL = \beta^2 \frac{1 - (p_4/p_1)^2}{\gamma M_1^2} + \left(\frac{\gamma + 1}{2\gamma} \right) \ln(p_4/p_1)^2 \quad , \quad (15)$$

which again differs from Darcy's equation by the logarithm term. This difference is also negligible except at small pressure ratios. It is interesting to note that equations (12) and (15) are identical to the isothermal results, equations (10b), when $\gamma = 1$.

Darcy's equation shows that β^2 can be absorbed into b in the incompressible case. In this case, only one constant, b/β^2 , characterizes the

gas-solid interaction. This is not surprising, since [5] develops a theory in which β does not enter explicitly. When compressibility becomes important this simplification is no longer possible and both b and β are separately significant parameters.

We have shown that Darcy's equation can be considered as the incompressible limit for both the isothermal and adiabatic cases, providing p_4/p_1 is not too small. An estimate of a lower limit for p_4/p_1 , denoted by $(p_4/p_1)_{\min}$, can be obtained by assuming the magnitude of the logarithm term is, say, 1/10 that of the other term. This results in

$$(p_4/p_1)_{\min} = \exp \left[- \frac{\beta^2}{10(\gamma + 1)M_1^2} \right], \quad (16)$$

where the $(p_4/p_1)^2$ quantity in the β^2 term has been neglected. For example, equation (16) results in $(p_4/p_1)_{\min} = 0.044$ when $\gamma = (7/5)$, $\beta = (1/2)$, and $M_1^2 = 0.001$. Hence, if $0.044 < (p_4/p_1)$, Darcy's equation can be used in place of equation (15), providing all Mach numbers are small. Equation (16) shows that small values of β/M_1 result in values of $(p_4/p_1)_{\min}$ near unity, in which case Darcy's equation is no longer useful.

A criterion for the use of incompressible flow theory can now be derived. In doing so, we approximate F by $1/\gamma M^2$ and freely use equations (7). Since the largest of the Mach numbers is M_3 , the flow is considered incompressible if $F(M_3^2) \geq 10$ or $M_3 \leq 0.239$ (see Fig. 7). From equation (13), we have

$$\frac{1}{\gamma M_3^2} = \frac{1}{\gamma M_2^2} - bL \geq 10 \quad ,$$

which, after some manipulation, results in

$$(p_4/p_1)^2 \geq (p_4/p_1)_{inc}^2 = \frac{1}{1 + (bL/10)} \quad (17)$$

The flow is thus approximately incompressible if (p_4/p_1) is greater than $(p_4/p_1)_{inc}$. This result should not be confused with (16), which concerns the relative importance of the logarithm term in equation (15).

The Compressible Momentum Equation

In the remainder of this paper, we deal only with the compressible, adiabatic result, equation (13). This equation, in conjunction with equations (2), shows that

$$bL = f_0(M_1^2, \beta, \gamma, p_4/p_1) \quad (18)$$

An important conclusion based on equations (1) and (18) is that for given values of β , γ , p_4/p_1 , and $p_1\rho_1$, the mass flow rate $\rho_1 u_1$ adjusts to conserve momentum. Any change in the flow rate through a plate thus requires a new p_4/p_1 . For fixed values of β , γ , and p_4/p_1 , an alternative interpretation is that momentum conservation relates M_1^2 and bL . In fact, this relation is single-valued as shown in the Appendix.

As noted earlier, the two Fanno curves coincide when $\beta = 1$. We therefore obtain the relation

$$f_0(M_1^2, 1, \gamma, p_4/p_1) = F(M_1^2) - F(M_4^2) \quad .$$

It is important, however, to note that

$$bL \neq F(M_1^2) - F(M_4^2) \quad , \quad (19)$$

when $\beta < 1$, since erroneous results are obtained if the two area changes are ignored. (Compare this with equation (13).) To demonstrate this more clearly, we determine

$$\frac{\partial(bL)}{\partial\beta} = \frac{\partial f_0}{\partial\beta} = \frac{dF(M_2^2)}{dM_2^2} \frac{\partial M_2^2}{\partial\beta} - \frac{dF(M_3^2)}{dM_3^2} \frac{\partial M_3^2}{\partial\beta} \quad ,$$

where conditions at 1 and 4 are held fixed. We obtain

$$\frac{\partial(bL)}{\partial\beta} = \frac{2}{\gamma\beta} \left\{ \frac{1}{M_2^2} - \frac{1}{M_3^2} \left[\frac{1 - M_3^2}{1 + (\gamma - 1 - \gamma\beta)M_3^2} \right] \right\} \quad ,$$

which is always positive. If instead, $(\partial bL/\partial\beta)$ had been zero, f_0 would not depend on β and an equality sign in (19) would be correct. Thus, the area changes cannot be ignored when dealing with conservation of momentum.

This is also evident from the fact that the average Mach number on the Fanno curve from 2 to 3 is greater than that on the Fanno curve from 1 to 4. The positive value of $(\partial bL/\partial\beta)$ means the product bL must increase if β increases, in order to maintain constant conditions at 1 and 4.

We conclude this section by examining the limit $M_3 \rightarrow 1$, with $M_4^2 = \overline{M_4^2}$ and $(p_1 M_1 / p_4)^2 = (\overline{p_1 M_1 / p_4})^2$. In this situation,

$$bL = f_1(M_1^2 / \beta^2, \gamma) = F(M_2^2) - F(1) \quad , \quad (20)$$

as is evident from equations (2b), (13), and (14). This result is shown as Fig. 8 for $\gamma = (7/5)$. Hence, for given values of γ (e. g., $7/5$), β , and p_4/p_1 we can determine bL such that $M_3 = 1$. To do this, first determine $\overline{M_4^2}$ by Fig. 4, then $(\overline{p_1 M_1 / p_4})^2$ by Fig. 5, and finally bL by Fig. 8.

We may, of course, specify γ , β , and bL and then determine a value for p_4/p_1 , denoted in accordance with our notation by $(\overline{p_4/p_1})$, such that $M_3 = 1$. Figure 9 shows $(\overline{p_4/p_1})^2$ versus bL for $\gamma = (7/5)$ and various values of β^2 , including $\beta = 1$. Values of p_4/p_1 greater than $(\overline{p_4/p_1})$ result in $M_3 < 1$; values less than $(\overline{p_4/p_1})$ are considered in the next section. All the curves in Fig. 9 are parallel because $(M_1^2 / \beta^2) = (\overline{p_4/p_1})^2 g$, where g is a function only of β and γ . The solid curve is for both $\beta = 0$ and $\beta = 1$. As β increases, $(\overline{p_4/p_1})$ at first increases, reaches a maximum at about $\beta = 0.6$, and then decreases to the $\beta = 1$ value. This behavior can be shown to be due to the curvature of the path that represents the 3 to 4 process, as shown in Fig. 2. The process twice intersects some constant pressure lines, thereby resulting a double-valued behavior for $(\overline{p_4/p_1})$. Since the curves are so close together, the pressure ratio for choking, $(\overline{p_4/p_1})$, is insensitive to β .

Finally, for large bL , i. e., for a thick plate, we have approximately

$$bL \approx \frac{1}{\gamma M_2^2} \approx \frac{\beta^2}{\gamma M_1^2} = \frac{\beta^2}{\gamma (p_4/p_1)^2 G_0(M_4^2)}$$

and hence $\ln(p_4/p_1)^2$ is proportional to $\ln bL$, as is evident from Fig. 9.

Note that $bL \approx (\beta^2/\gamma M_1^2)$ is essentially Darcy's equation when p_4/p_1 is small.

CHOKED FLOW: $M_3 = 1$.

When $(p_4/p_1) < (\overline{p_4/p_1})$, equations (2c), (3), (4), and (5) no longer apply, and state 4 cannot be directly related to state 3 as before. These equations are replaced by $M_3 = 1$, and conditions at 1, 2, and 3 are unaffected by changes in p_4 . Since conditions at 1 and 2, as determined by equations (2b) and (20), are fixed, we concentrate on conditions at 4, where M_4 is determined by equation (2a).

The analysis is again conveniently illustrated by a Mollier diagram (Fig. 10). State points 1, 2, and 3 are the same as in Fig. 2, except that 3 is at the "nose" of the Fanno curve. The limit $M_3 \rightarrow 1$, is shown as $\overline{4}$. For pressure ratios slightly less than $(\overline{p_4/p_1})$, state 4 is to the right of $\overline{4}$ on the Fanno curve through state 1. State 4 thus moves in a continuous manner along the Fanno curve as p_4/p_1 decreases.

If p_4 is further decreased, state 4 is at the "nose" of the curve where $M_4 = 1$, and the corresponding pressure ratio is designated by $(p_4/p_1)^*$. A further decrease in p_4/p_1 results in supersonic flow, since $M_4 > 1$. For a sufficiently small pressure ratio, denoted by $(\underline{p_4/p_1})$, conditions at 4 are reached by an isentropic expansion from 3 to $\underline{4}$, as shown in Fig. 10. Solutions do not exist for pressure ratios smaller than $(\underline{p_4/p_1})$, which is referred to as the limiting pressure ratio.² This limit results from our

²This limiting pressure ratio probably cannot be attained in practice due to the effects of turbulence downstream of the plate. A smaller downstream reservoir pressure than the limiting one should result in a flow at the end of the duct analogous to the flow external to an underexpanded nozzle.

insistence on a constant-area duct. A smaller pressure ratio, for example, requires an expanding flow and an increasing duct cross-sectional area downstream of the plate.

It should be realized that the flow may be quite turbulent downstream of the plate. In this situation, state 4 does not occur until a uniform duct flow is achieved. Thus, state 4 is frequently downstream of the plate rather than at its surface.

Conditions at 4, when

$$\underline{(p_4/p_1)} \leq (p_4/p_1) \leq \overline{(p_4/p_1)}$$

are determined by combining equations (2a), (2b), and (13) to yield

$$F(M_2^2) = bL + F(1) \quad , \quad (21a)$$

$$M_4^2 = \frac{1}{(\gamma - 1)} \left\{ \left[1 + 2(\gamma - 1)(p_1/p_4)^2 \beta^2 G_1(M_2^2) \right]^{1/2} - 1 \right\} \quad . \quad (21b)$$

Thus, M_4 depends only on γ , bL , and $(p_1 \beta / p_4)$. The pressure ratio $(p_4/p_1)^*$, as a function of bL , γ , and β , is obtained by setting $M_4 = 1$. Figure 9 shows $[(p_4/p_1)^*]^2$ versus bL for $\gamma = (7/5)$ and various β^2 , including $\beta = 1$. As with $\overline{(p_4/p_1)}$, these curves are also parallel. One difference, however, is that decreasing β results in a smaller $(p_4/p_1)^*$ for a fixed bL . This is evident once it is realized that decreasing β separates the Fanno curves, while a constant bL means that the Fanno curve through 2 is kept fixed.

The Mach number \underline{M}_4 at the limiting pressure ratio is determined by the isentropic relation

$$G_1(\underline{M}_4^2) = [2/(\gamma + 1)]^{(\gamma+1)/(\gamma-1)} \beta^2$$

where equations (21) still apply. These may be solved for $(\underline{p}_4/\underline{p}_1)$, which is also shown in Fig. 9 for $\gamma = (7/5)$ and various β^2 , including $\beta = 1$. The variation of $(\underline{p}_4/\underline{p}_1)$ with β is much greater than for the other pressure ratios shown in Fig. 9. We also see that all the curves are again parallel.

Basically, this occurs because the same momentum equation (13) and Fanno curve equation (2a) apply to all the curves.

DISCUSSION

Three principal topics are discussed in this section, all of which bear on experimental verification. First, the various flow regimes are described in terms of the pressure ratio. An appropriate generalization of the volumetric flow rate versus pressure differential plot is then given. The third topic is a discussion of the physical implications of the drag coefficient b .

There are four flow regimes that can be characterized by the pressure ratio p_4/p_1 . The first is

$$(p_4/p_1)_{inc} \leq (p_4/p_1) \leq 1$$

where $(p_4/p_1)_{inc}$ is given by equation (17). This is the incompressible regime where Darcy's equation is usually valid. The next regime

$$\overline{(p_4/p_1)} \leq (p_4/p_1) < (p_4/p_1)_{inc}$$

is characterized by compressible subsonic flow everywhere. The third regime

$$(p_4/p_1)^* \leq (p_4/p_1) < \overline{(p_4/p_1)}$$

requires a choked flow, with subsonic flow at 4. The final regime

$$\underline{(p_4/p_1)} \leq (p_4/p_1) < (p_4/p_1)^*$$

also requires a choked flow, with supersonic flow downstream of the plate.

Of the four regimes, there can be no doubt about the characteristics of the first.

The others still require experimental verification. This is particularly true of the last, since supersonic flow has not, as yet, been associated with flow through a porous medium. This regime may be the easiest to verify, however, since standard techniques, such as the Schlieren optical method, can be used to detect the presence of supersonic flow downstream of the plate.

Incompressible flow through a porous medium is frequently represented by a linear relation between the volumetric flow rate and the pressure differential. This representation does not hold for compressible flow. More appropriate would be a plot of M_1^2 versus $(p_4/p_1)^2$, as shown in Fig. 11. (Once M_1 and (p_4/p_1) are known, M_4 is readily determined by equation (2a).) This figure is for $\beta^2 = 0.2$, $\gamma = (7/5)$, and various bL . The solid curves are for compressible flow, where the (Δ) denotes the pressure ratio $(p_4/p_1)_{inc}$, and the (o) denotes the onset of choking. These curves terminate at (p_4/p_1) . The dashed line is the incompressible result, equation (15), while the doubly dashed line is Darcy's equation, which differs from (15) when $(p_4/p_1) \leq (p_4/p_1)_{min}$. This difference shifts to smaller pressure ratios as bL increases in accordance with (16).

For bL equal to 1 and 10, we see that the compressible and incompressible results depart at $(p_4/p_1)_{inc}$. For bL equal to 10^2 and $(p_4/p_1)^2 < 0.1$, only small changes in M_1^2 are necessary for large changes in M_3 and p_4/p_1 . Since this is true for both the incompressible and compressible results, the two remain quite close. For a thick plate, i. e., large bL , Darcy's equation adequately predicts M_1^2 versus $(p_4/p_1)^2$, as noted earlier. The incompressible solution does not, of course, correctly predict M_4 or (p_4/p_1) .

Experimental data will not necessarily follow a single bL curve as flow conditions vary. Deviations occur because b generally varies with flow conditions. It is therefore necessary to explore the relationship of b to the other parameters of the problem, since experimental verification depends to some extent on this relationship.

Any experimental investigation must deal with at least three types of parameters. The first are those that characterize the gas, such as γ and the viscosity. The second are those that characterize the porous medium, such as β . Finally, there are parameters associated with the specific flow situation, such as $\rho_1 u_1$. All parameters used so far, except b , have a straightforward physical interpretation and are experimentally determinable. Part of the difficulty with b is that it depends on the gas, porous medium, and flow conditions. This is evident from the relation $b = (2\eta/\rho u B_0)$ given earlier.

The drag coefficient was introduced with the expectation that it is independent of β , which must be specified as well. In addition, it is reasonable to expect that b does not depend on the molecular weight of the gas or on γ . The first exclusion stems from dimensional analysis, while the second is due to the explicit appearance of γ in the theory. In order to define more clearly the role of b , we proceed by comparing the flow in a porous medium with that in a pipe with roughened walls. This type of comparison is subject to criticism, as [1] points out, and our conclusions are, at best, heuristic. We nevertheless briefly pursue this course in order to introduce concepts that may be experimentally useful.

According to this analogy, b should depend on some average pore diameter d (or equivalently on the specific surface), and on the Reynolds number $R_d = (\rho_1 v_1 d / \eta_1)$. Thus, $b = (2d/B_0 R_d)$ and if d/B_0 is constant, b is inversely proportional to the Reynolds number, a result typical of laminar flows. For sufficiently large values of R_d , however, due to turbulence, d/B_0 is not necessarily constant. The drag coefficient may also depend on the Mach number, although this dependence is believed to be weak (see [4], Chapter 6). For a specific medium, b may also change with time due to surface changes such as adsorption. In addition, b may depend strongly on certain characteristics of the material, such as the relative roughness (see [4], Chapter 6). For sufficiently large flow rates, the flow is not only turbulent, but b may be nearly independent of R_d . In this circumstance, b depends primarily on the relative roughness alone. This regime is ideal for experimentally verifying this analysis, providing it occurs before the flow chokes.

Even if b does not have precisely the behavior described above, experimental verification is still possible. For example, use can be made of the fact that once choking has occurred, the flow from 2 to 3 does not change and bL remains constant.³ Furthermore, in the compressible regime when $M_3 < 1$, problems associated with b might be avoided by using different plate thicknesses of the same porous material. For engineering purposes, plots of b versus the pertinent parameters, such as R_d , are of course necessary.

³We are, of course, allowing only p_4 to vary.

In conclusion, note that although we have dealt exclusively with the pressure and Mach number, other quantities are easily determined. For example, the temperature at 4 is known for all flow situations from

$$\frac{T_1}{T_4} = 1 + \left(\frac{\gamma - 1}{2}\right) M_4^2 ,$$

since the stagnation temperature, approximately given by T_1 , is a constant. Another useful quantity is the stagnation pressure p_0 . At 1 this is approximately equal to p_1 , but at 4 it is

$$\frac{p_{04}}{p_4} = \left[1 + (\gamma - 1) M_4^2 / 2 \right]^{\gamma / (\gamma - 1)} ,$$

and consequently, $(p_4/p_1) < (p_{04}/p_{01})$. This difference in static and stagnation pressure ratios is not necessarily small, e. g., with $\gamma = (7/5)$ and $M_4 = 1$ we have $(p_{04}/p_{01}) = 1.892 (p_4/p_1)$.

REFERENCES

1. A. E. Scheidegger, The Physics of Flow Through Porous Media, University of Toronto Press (1960).
2. P. C. Carman, Flow of Gases Through Porous Media, Butterworth Scientific Publications, London (1956).
3. R. A. Hartunian and D. J. Spencer, Visualization Technique for Massive Blowing Studies, AIAA J. 4, 1305 (1966).
4. A. H. Shapiro, The Dynamics and Thermodynamics of Compressible Fluid Flow, Vol. 1, The Ronald Press Co., New York (1953).
5. J. P. Jones, The Propagation of Elastic Waves in a Porous, Saturated, Elastic Solid, Ph. D. Thesis, Purdue University (1964).

APPENDIX

If $(\partial bL / \partial M_1^2)$ is non-zero, then bL and M_1^2 are uniquely related. This derivative is [see equation (18)]

$$\frac{\partial(bL)}{\partial M_1^2} = \frac{\partial f_0}{\partial M_1^2} = \frac{dF(M_2^2)}{dM_2^2} \frac{\partial M_2^2}{\partial M_1^2} - \frac{dF(M_3^2)}{dM_3^2} \frac{\partial M_3^2}{\partial M_4^2} \frac{\partial M_4^2}{\partial M_1^2} ,$$

where the derivatives, such as $(\partial M_2^2 / \partial M_1^2)$, are determined by equations (2) and (4). We thus obtain

$$\frac{\partial(bL)}{\partial M_1^2} = - \frac{1}{\gamma M_1^2} \left(\frac{1}{M_2^2} - \frac{H}{M_3^2} \right) ,$$

where

$$H(M_3^2) \equiv \frac{(1 - M_3^2) (1 + \gamma \beta M_3^2) (1 - M_4^2)}{[1 + (\gamma - 1 - \gamma \beta) M_3^2] (1 + \gamma M_4^2) [1 + (\gamma - 1) M_4^2]} ,$$

and M_3^2 and M_4^2 are related by equation (4). It is easy to see that $H(0) = 1$ and $H(1) = 0$. One can also show that $(dH/dM_3^2) \leq 0$ for $0 \leq M_3 \leq 1$. Consequently, $H \leq 1$ and since $M_2 < M_3$, we have $(\partial bL / \partial M_1^2) < 0$, and bL and M_1^2 are uniquely related. Furthermore, since $(\partial bL / \partial M_1^2)$ is negative, increasing M_1^2 means bL must decrease if p_4/p_1 is to remain constant. In other words, we get the result that if the pressure ratio p_4/p_1 is to remain constant as the mass flow rate is increased, the dimensionless product (bL) must decrease.

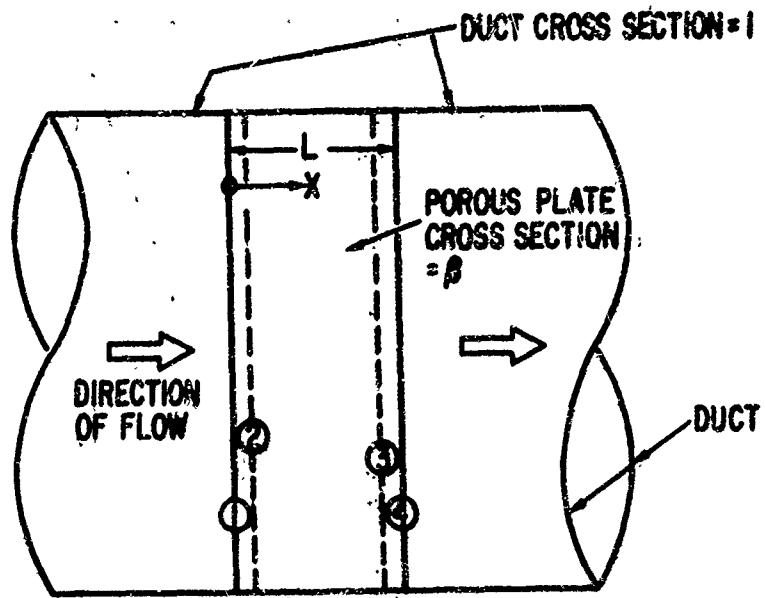


Fig. 1. Flow Schematic for a Porous Plate inside a Duct

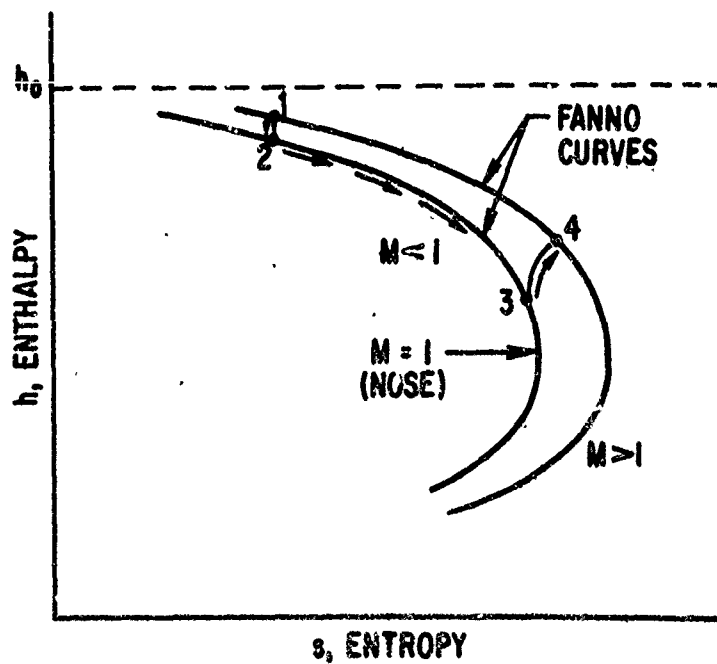


Fig. 2. Mollier Diagram for Subsonic Flow through a Porous Plate

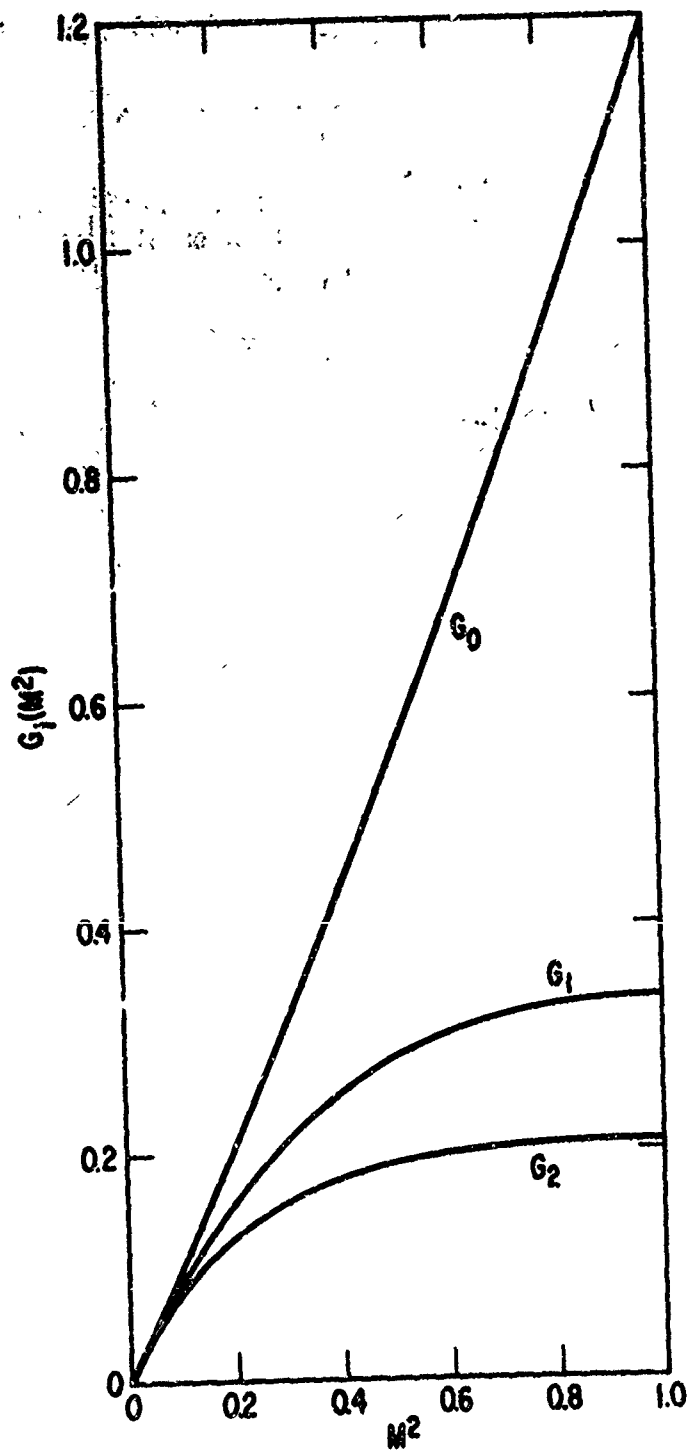


Fig. 3. $G_i(M^2)$ vs M^2 ; $\gamma = 7/5$

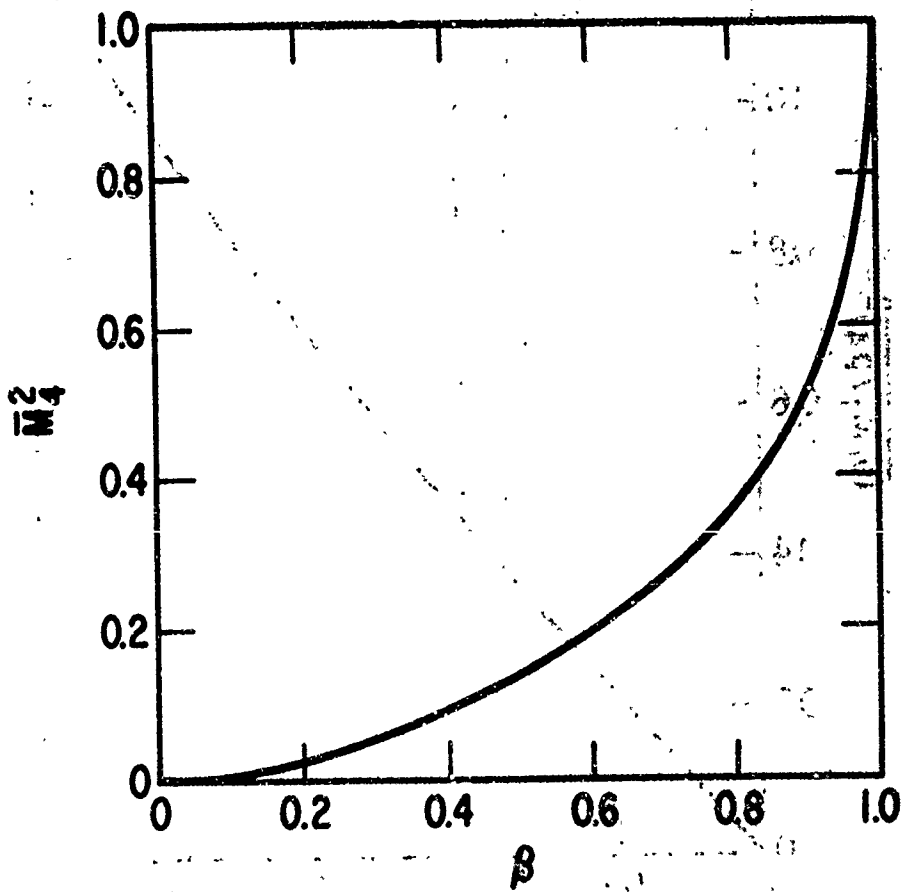


Fig. 4. \overline{M}_4^2 vs β ; $\gamma = 7/5$

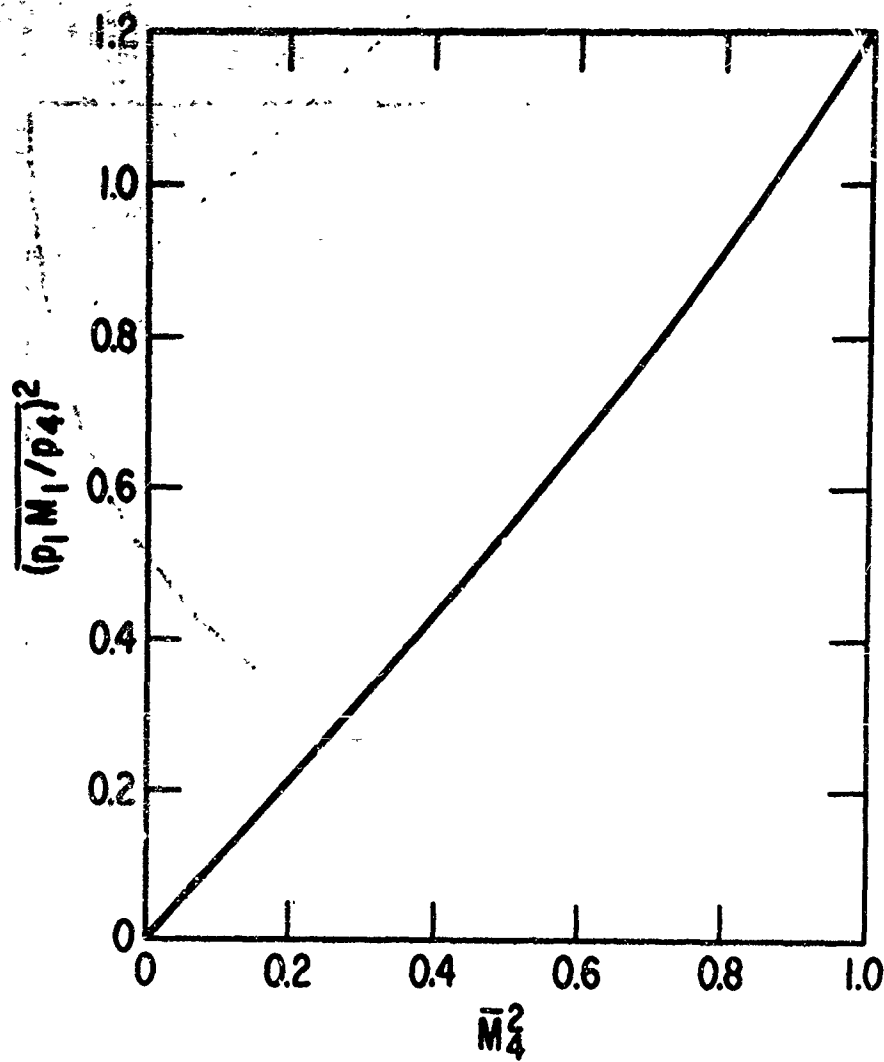


Fig. 5. $(p_1 M_1 / p_4)^2$ vs \bar{M}_4^2 ; $\gamma = 7/5$

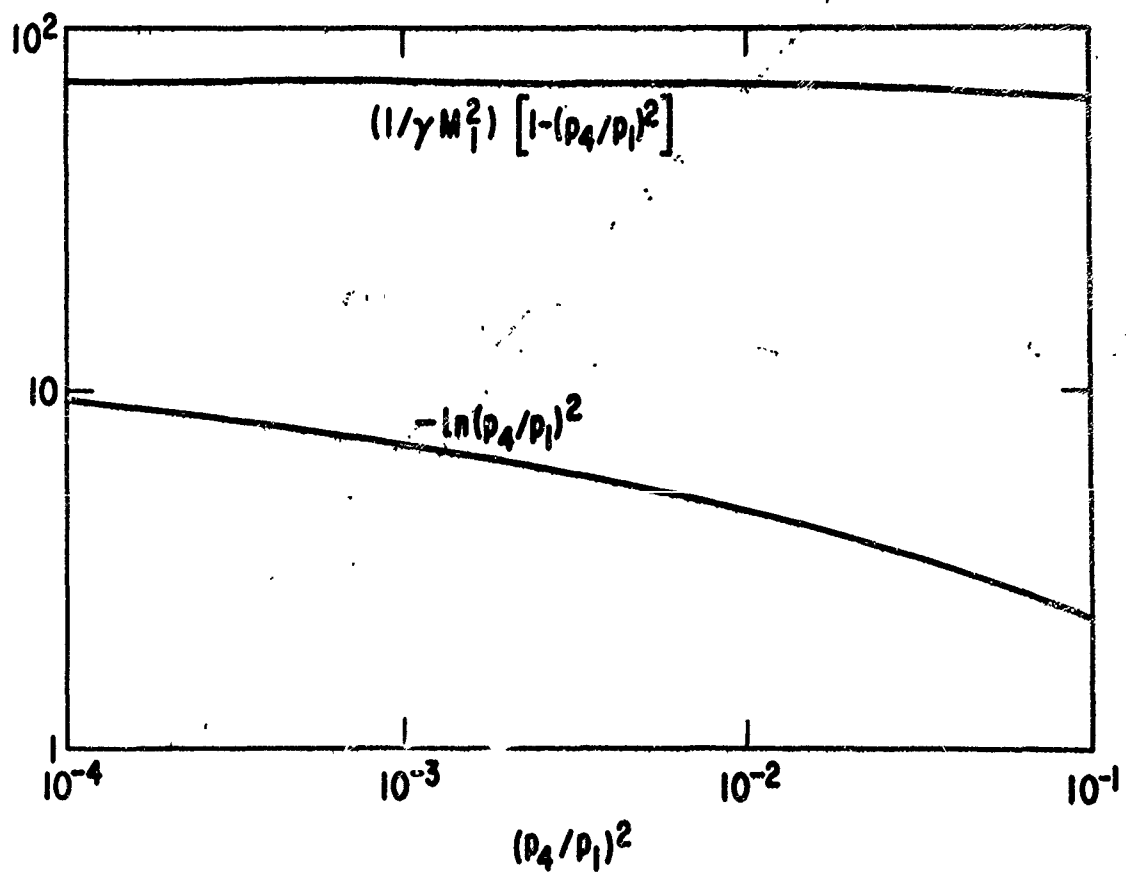


Fig. 6. Comparison of the Terms in Equation (10b);
 $\gamma = 7/5, M_1^2 = 0.01$

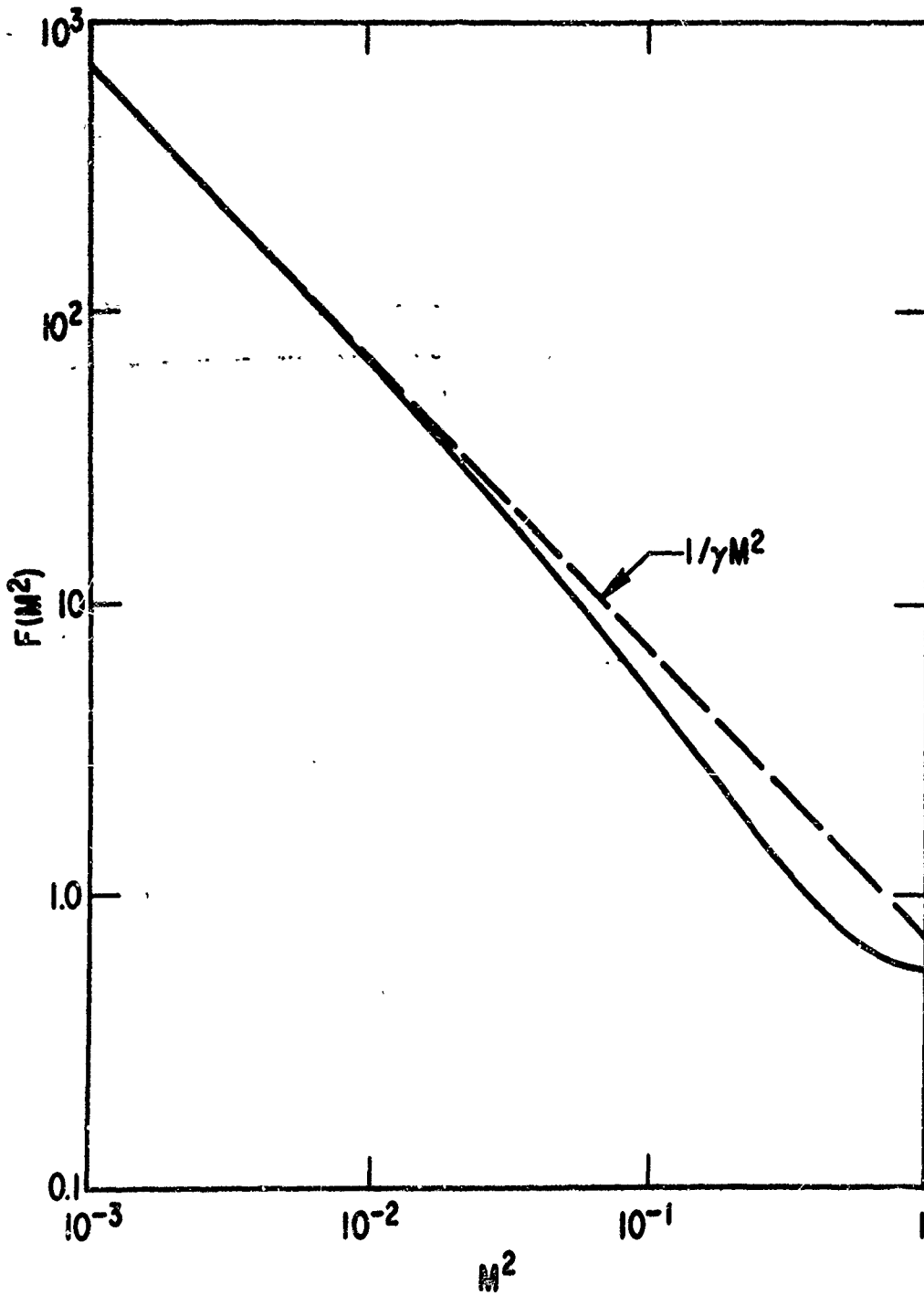


Fig. 7. $F(M^2)$ vs M^2 ; $\gamma = 7/5$

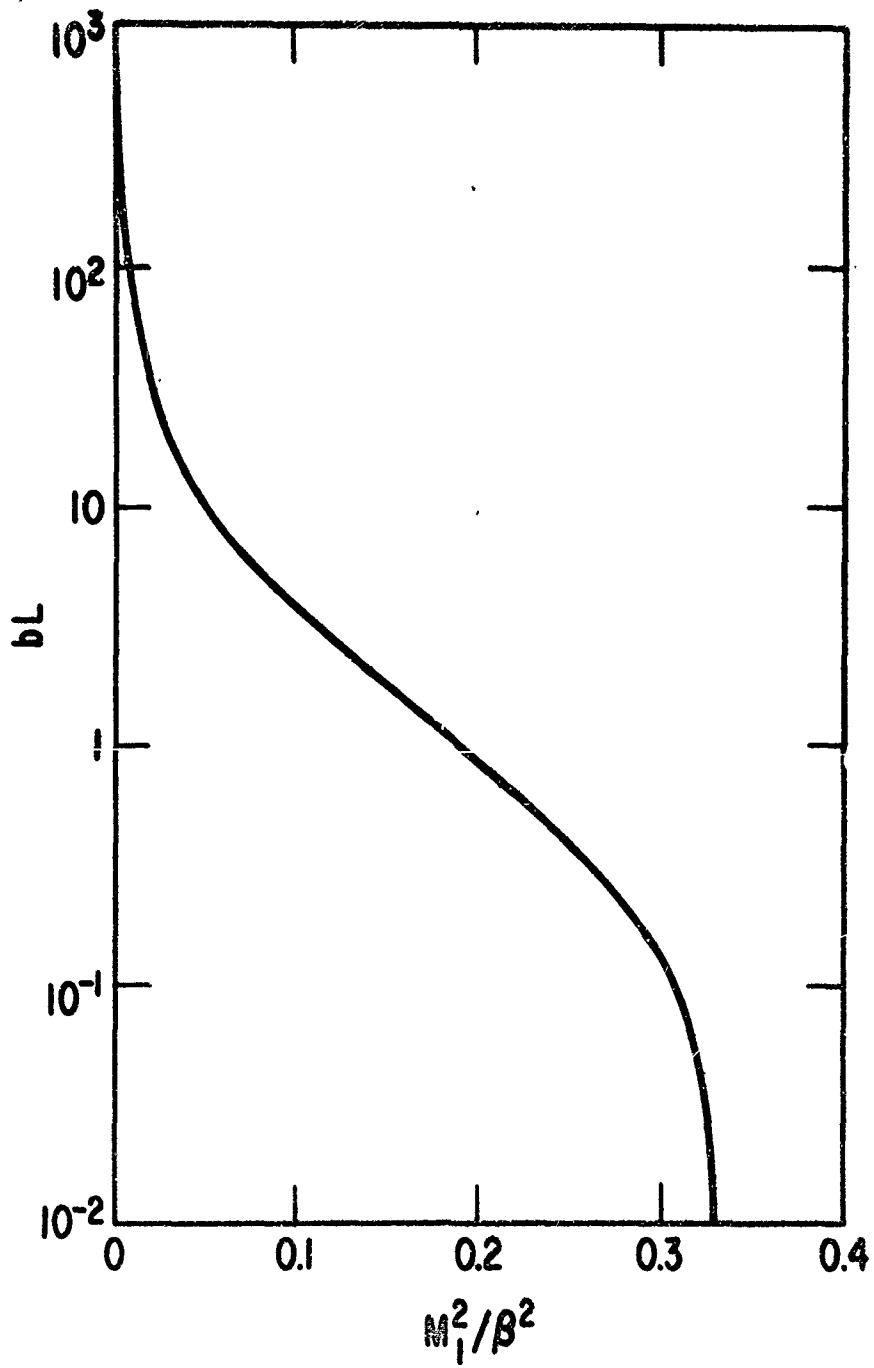


Fig. 8. bL vs M_1^2/β^2 when $M_3 = 1$; $\gamma = 7/5$

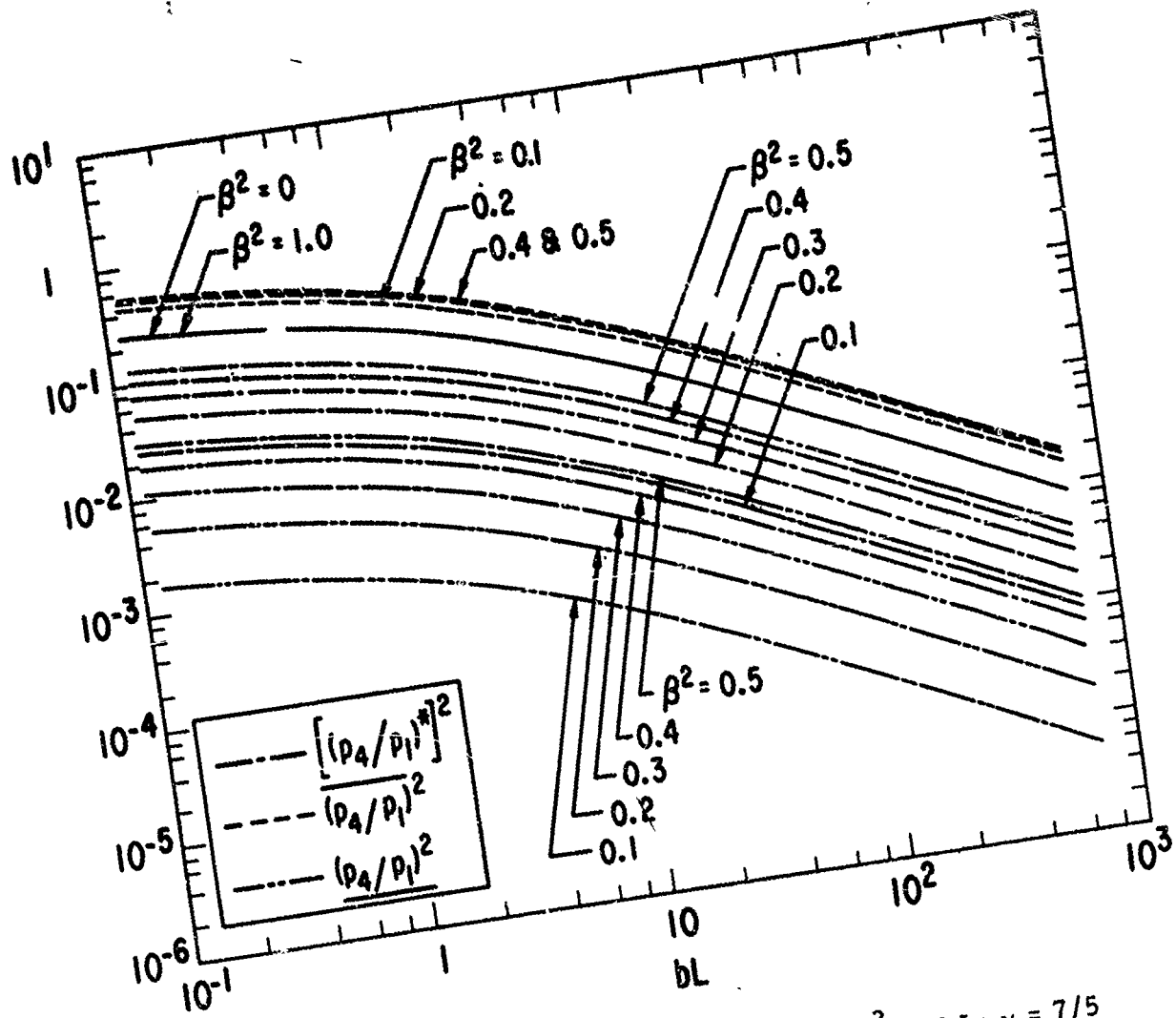


Fig. 9. $(p_4/p_1)^2$, $[(p_4/p_1)^*]^2$, and $(p_4/p_1)^2$ vs bL ; $\gamma = 7/5$

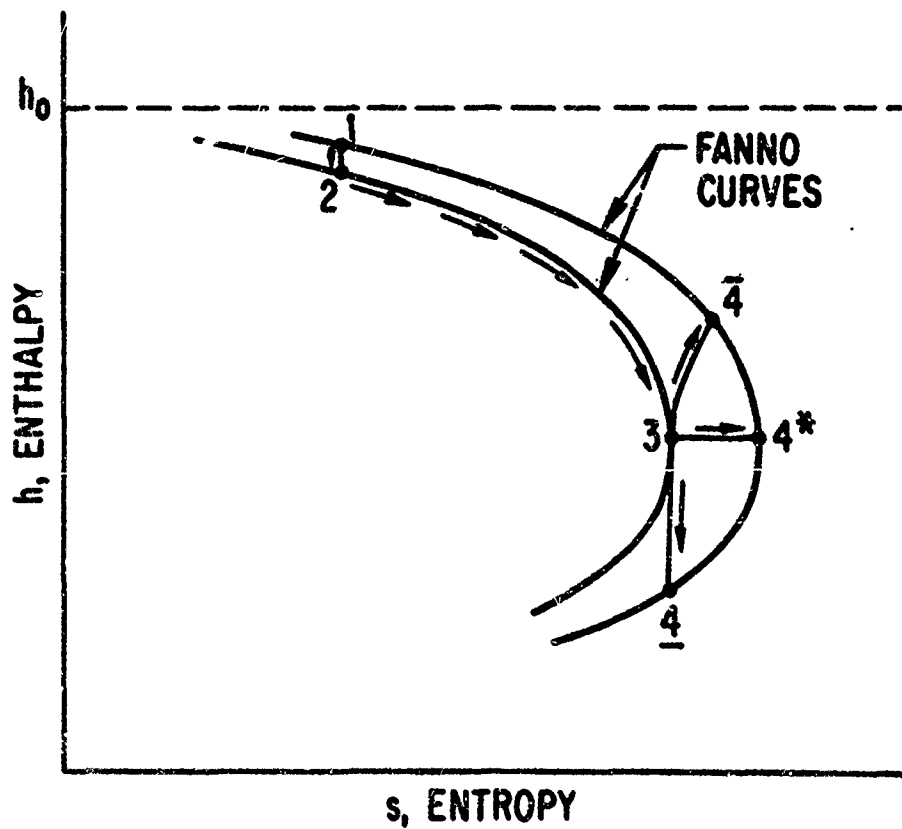


Fig. 10. Mollier Diagram for Choked Flow Through a Porous Plate

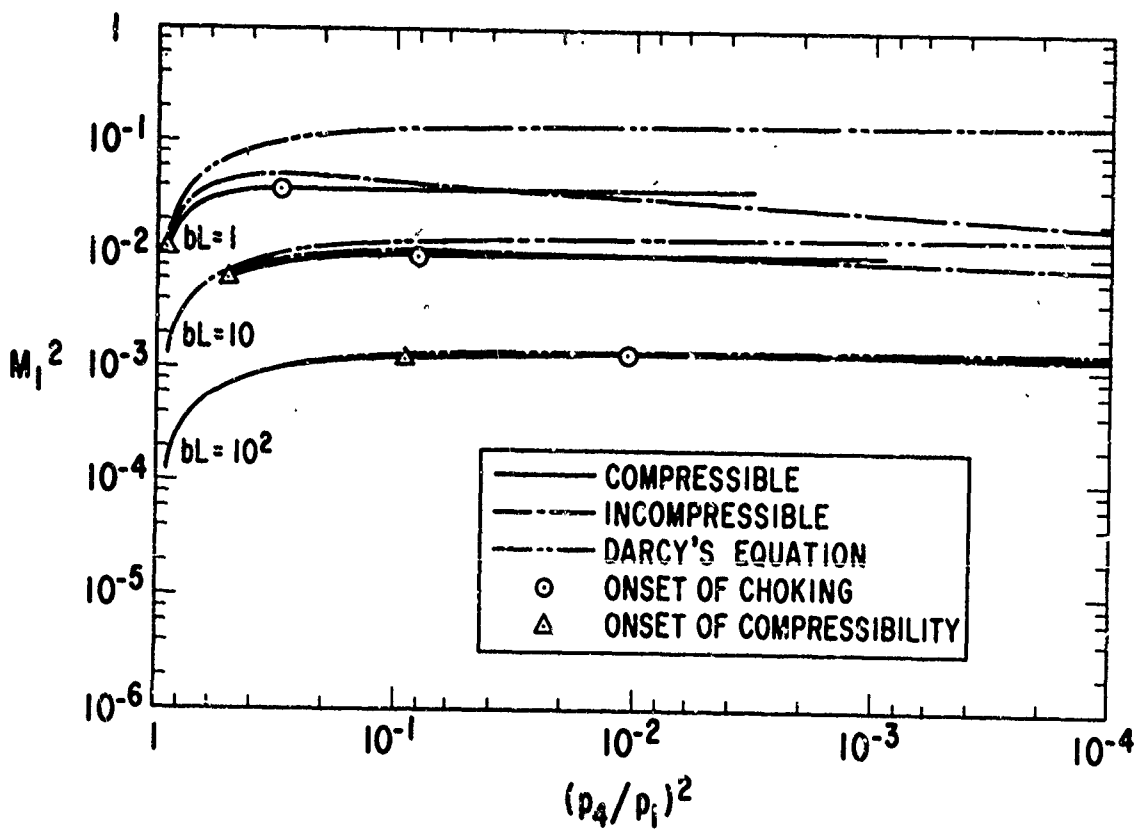


Fig. 11. M_1^2 vs $(p_4/p_1)^2$ for $bL = 1, 10, 10^2$; $\beta^2 = 0.2$; $\gamma = 7/5$

UNCLASSIFIED
Security Classification

DOCUMENT CONTROL DATA - R&D

(Security classification of title, body of abstract and indexing annotations must be entered when the overall report is classified)

1. ORIGINATING ACTIVITY (Corporate author) Aerospace Corporation El Segundo, California		2a. REPORT SECURITY CLASSIFICATION Unclassified	
		2b. GROUP	
3. REPORT TITLE Compressible Flow Through a Porous Plate			
4. DESCRIPTIVE NOTES (Type of report and inclusive dates)			
5. AUTHOR(S) (Last name, first name, initial) Emanuel, George and Jones, John P.			
6. REPORT DATE August 1966		7a. TOTAL NO. OF PAGES 42	7b. NO. OF REFS 5
8a. CONTRACT OR GRANT NO. AF 04(695)-669		8c. ORIGINATOR'S REPORT NUMBER(S) TR-669(6240-20)-15	
b. PROJECT NO.		8d. OTHER REPORT NO(S) (Any other numbers that may be assigned this report) SSD-TR-66-165	
c.			
d.			
10. AVAILABILITY/LIMITATION NOTICES This document is subject to special export controls, and each transmittal to foreign governments or foreign nationals may be made only with prior approval of SSD(SSRT).			
11. SUPPLEMENTARY NOTES		12. SPONSORING MILITARY ACTIVITY Space Systems Division Air Force Systems Command Los Angeles, California	
13 ABSTRACT A simple one-dimensional theory is given for the steady, compressible, adiabatic flow of a perfect gas through a porous plate. The Dupuit-Forchheimer relation, valid for incompressible flow, is replaced by an isentropic compression when the gas enters the plate and a non-isentropic sudden enlargement process when it exits. A generalized form of Darcy's equation is used that is applicable to adiabatic flow. It retains the convective term, which is necessary if the flow is compressible. An important consequence of this study is that the Mach number at the downstream surface may be much smaller than unity, even when the flow through the plate is choked. As the pressure ratio across the plate decreases, the flow remains choked, but the downstream Mach number increases. In fact, this Mach number will be greater than unity for a sufficiently small pressure ratio, in which case the downstream flow is supersonic. Thus, a wide range of downstream Mach numbers from subsonic to supersonic is possible, even though the flow is choked. For incompressible flow, the volumetric flow rate varies linearly with the pressure differential across the plate. The equivalent compressible relation is shown to consist of a plot of upstream Mach number versus the pressure ratio across the plate. The incompressible result can also be shown on this plot, it differs from the compressible one, except when the plate is thick.			

UNCLASSIFIED

Security Classification

KEY WORDS

Steady, one-dimensional, compressible flow
Porous Plate
Dupuit-Forchheimer equation
Darcy's equation
Fanno curve
Subsonic, supersonic flow

Abstract (Continued)

UNCLASSIFIED
Security Classification